BIOCHEMICAL AND BIOPHYSICAL RESEARCH COMMUNICATIONS **252,** 166–172 (1998)
ARTICLE NO. RC989584

Characterization of a Cytochrome P450 from the Acidothermophilic Archaea *Sulfolobus solfataricus*

Mark A. McLean, Shelley A. Maves, Kara E. Weiss, Scott Krepich, and Stephen G. Sligar[1]
Beckman Institute for Advanced Science and Technology, University of Illinois, Urbana, Illinois 61801

Received September 30, 1998

We report the cloning, expression, purification, and molecular characterization of a cytochrome P450 (CYP119) from the thermophilic archaea *Sulfolobus solfataricus*. This protein displays an absorption spectra in the reduced, oxidized, and carbonyl adduct analogous to those of other P450 enzymes. We demonstrate that P450 (CYP119) exhibits remarkable thermo- and pressure stability, with a melting temperature 40° higher than that of the extensively studied cytochrome P450cam (CYP101) and an optical spectra completely resistant to the formation of the inactive P420 by hydrostatic pressure up to 2 kbar. CO flash photolysis experiments, as well as construction of a CYP119 homology model, suggest an open active site with greater solvent access than P450 (CYP101) and similar to that of P450 (CYP102). This communication represents the first molecular characterization of an extremophilic cytochrome P450.

Cytochromes P450 are a superfamily of enzymes which perform many important biological oxidations. These enzymes contain a iron protoporphyrin IX prosthetic group which catalyzes the cleavage of bound molecular oxygen and formation of an oxygenated product. It is this specialized functionality that makes the P450s unique amongst the cytochromes. P450s are found in a broad range of species including bacteria, plants, fungi, insects and mammals. Numerous types of reactions are carried out by P450s including very selective regio- and stereo-specific hydroxylations (1) resulting in commercially relevant products such as pesticide resistant plants and drug precursors. Unfortunately the stability of many of these P450 enzymes does not allow for the construction of an efficient bioreactor. The understanding of the structural elements that make a protein thermostable is still very limited so that predicting what types of mutations are needed in an enzyme to make it more stable is problematic.

Recently a gene in archaebacteria *Sulfolobus solfataricus* (*Ss*) has been identified which encoded for a P450, the first known in the Archea philogenetic domain (2). *Sulfolobus solfataricus* is an acidothermophilic archaea which has an optimum growth temperature of 85°C. Several proteins have already been characterized from *Ss* such as beta glucosidase and ribonuclease P2 (3, 4). Some of the enzymes from this bacteria have shown extreme stability towards elevated hydrostatic pressure in addition to the high thermostability exhibited. For example, ribonuclease P2 is an extremely pressure/themostable protein from *Ss* which does not unfold until pressures are greater than 14 kbar and temperatures >360 K (4). Interestingly enough, a single point mutation (Phe31Ala) in the hydrophobic core of ribonuclease P2 lowers the midpoint of the denaturation curve to 4 kbar. Phe 31 lies in an aromatic cluster in the center of the protein. Disruption of this interaction leads to a dramatic decrease in pressure stability while the Phe31Tyr mutant shows stability similar to wild type enzyme (4). This implicates an important role for aromatic stacking clusters contributing to pressure stabilization.

Characterization of other *Ss* proteins has offered additional possibilities for the origin of their stability. *Ss* contains an iron superoxide dismutase (SOD) which is stable, with a half life of 2 h, at 100°C (5). The peptide sequence of *Ss* SOD contains a higher average hydrophobic content and molecular weight compared to the non-thermophilic SODs which has been suggested to be linked to thermostability. A comparison of β-glycosidase isolated from almond to that found in *Ss* also corroborates the existence of increased hydrophobicity as well as increased rigidity as a source for thermostability (6). Another idea suggested by some studies is that thermostability and barostability may be linked. In a study of carboxypeptidase from *Ss* it is noted that at elevated pressures the thermostability of this enzyme increases whereas similar carboxypeptidases from non-thermophilic organisms do not display this behavior (7).

[1] To whom correspondence should be addressed.

0006-291X/98 $25.00

Since cytochromes P450 carry out many important, and possibly commercially relevant, chemical reactions it is critical to understand what structural features convey thermo- and barostability. To this end we have cloned and isolated the first thermo/barostable P450 from *Sulfolobus solfataricus*. We have used sequence alignments to P450s of known structures to generate a homology model from which we discuss the possible stabilizing factors. Several aspects of this model of the P450 (CYP119) structure are verified by physical measurement.

MATERIALS AND METHODS

Construction of pKS119. *Sulfolobus solfataricus* was purchased from ATCC (Strain #35091) and cultures were grown in medium 1304 (ATCC) at 75°C. Chromosomal DNA was isolated by standard procedures (8). The genomic DNA was digested with restriction endonuclease *Eco*RI followed by PCR to amplify the CYP119 gene. The oligonucleotide primers for PCR were synthesized at the University of Illinois Biotechnology center using the N-terminal primer 5′-TATCTATTTAGAATTCCGTTCCAGGAGACAACAACAATGTATGACTGGTTTAGTGAGATGAGAAAGAAAGACCCAGTGTATTATGAC-3′ and C-terminal primer 5′-GAGAAACCTCGGATCCTTATTCATTACTCTTCAACCTGACCACTAGTCTCTTATAACCATTCA-3′ sequences of the CYP119 gene. The 5′ end of the N-terminal primer contained additional bases to add a ribosome binding site. The PCR product was digested with *Eco*RI and *Bam*HI and ligated into the polylinker region of puc18 behind the lac promoter. The resulting product was transformed into *E. coli* TB-1 cells and selected for ampicillin resistance.

Expression and purification of CYP119. Overnight cultures of *E. coli* TB-1 harboring pKS119 were grown in 50 mL of LB (10 g tryptone/5 g yeast extract/10 g NaCl per liter) containing 0.2 g/L ampicillin at 37°C. 10 mL of this culture was used to inoculate a 1-L starter culture using 2× YT media (16 g tryptone/10 g yeast extract/5 g NaCl per liter) containing 0.2 g/L ampicillin. The starter culture was incubated at 37°C with shaking until it reached log phase (2–4 h). After reaching log phase 640 mL of the starter culture was used to inoculate 64 L of 2 ×YT media containing 0.2 g/mL ampicillin. The growth was allowed to proceed at 37°C/200 RPM for 18–20 h. Cells were harvested with a Beckman Instruments J2-21 centrifuge equipped with a continuous flow rotor. The resulting cell paste was weighed and then frozen at −70°C until use.

Total protein concentrations at each step in the purification were determined by the BCA protein assay from Pierce Chemical (Rockford, IL) according to manufacturer's protocols. The visible extinction coefficients were determined by extracting measuring the total amount of heme present in a pure sample using the pyridine hemochromagen assay (9) and comparing to the spectra obtained for the intact protein. Errors for reported extinction coefficients are ±10% Total P450 concentrations were determined by the CO bound minus oxidized UV-VIS spectra with $\epsilon_{450-490\ nm} = 91\ mM^{-1}$.

The *E. coli* cells were thawed and resuspended in 4 vol (4 mL/g cell paste) of 50 mM Tris–HCl pH 8.0 1 mM EDTA, 4 mg/mL lysozyme, 16 units/mL DNase, and 4 units/mL RNase. The cells were allowed to stir at 4°C for 4 h. to ensure complete lysis. Cell debris was removed by centrifugation at 30,000 rpm for 20 min. The supernatant was heated to 75°C for 15 min and then the unwanted denatured proteins were removed by centrifugation at 8000 rpm for 30 min, retaining the supernatant containing CYP119. An ammonium sulfate precipitation was performed first at 40% in which the CYP119 remains soluble and then 60% where the protein precipitates. The ammonium sulfate pellet was resuspended in a minimal volume of 10 mM Kpi, pH 7.2. The protein sample was fractionated on a Bio-Rad P-100 gel filtration column equilibrated in 10 mM Kpi, pH 7.2 and fractions containing the highest A_{415}:A_{280} ratio were pooled. The pooled fractions were injected onto a waters DEAE HPLC column and eluted with a 10 to 100 mM KPi gradient at pH 7.0. Cytochrome P450cam was purified as previously described (10).

UV–VIS spectroscopy. All spectra were recorded on a Hitachi U3300 spectrophotometer with a spectral bandpass of 1 nm. The spectra of the reduced protein was obtained by the addition of 10× molar ratio dithionite in an oxygen free environment and incubating for 20 min. Excess dithionite was removed by passing the sample over a G-25 column equilibrated in 100 mM Kpi, pH 7.0 all under anaerobic conditions. The reduced CYP119 was then sealed in a quartz cuvette with a Teflon stopper and placed in the spectrophotometer equilibrated at 4°C. A spectra of the reduced protein was recorded. To obtain the oxy-bound spectra the sample was opened to the air and a spectra was immediately recorded. The CO bound spectra was obtained by passing CO gas through the sample for 5 min and then adding a small excess of dithionite.

Differential scanning calorimetry. The MCS DSC unit from Microcal (Northhampton, MA) was employed for all experiments. CYP119 was exchanged into 100 mM Kpi, pH 7.0, by passage over a Sephadex G-25 gel-filtration column. Substrate free cytochrome P450cam was prepared by passage over a G-25 column equilibrated in 100 mM Tris–HCl, pH 7.5. The sample was concentrated and then passed over another G-25 column this time equilibrated in 100 mM Kpi, pH 7.0. DSC scans were taken with a scan rate of 70°C/h from 25 to 100°C for CYP119 and 25 to 80°C for P450cam.

High pressure spectroscopy. Spectra of the carbon monoxide bound forms CYP119 and P450cam using a Cary 3 spectrophotometer equipped with a pressure bomb previously described (11). Spectra were recorded from ambient pressure to 2.0 kbar at 0.5-kbar intervals.

CO flash photolysis. CO flash photolysis was performed as described elsewhere (12) with the following modifications. A logarithmic time base was used to collect data. This was achieved by utilizing two digital oscilloscopes each acquiring 25,000 points. The first records the data from 1 nanosecond to 2 μs while the second records data from 2 μs to 20 ms. The data are then binned using the following equation which results in a log time base with 40 points/decade: $t_i = t_0 \times 10^{0.025\ I}$ where i = 1 to 320 (8 decades, 40 points each) (13).

Homology modeling. The CYP119 sequence was aligned to the four P450 sequences with known crystal structures (CYP 107A, CYP 108, CYP101 and CYP102) (14-17) using the program Clustal W (18) and applying constraints imposed by the known structural information to obtain a multiple sequence alignment. Of the four known structures, CYP119 is most homologous to CYP 107A and CYP 108 (29 and 24% sequence identity and 48 and 39% similarity, respectively), therefore they were used as templates to build the molecular model. The homology model was then generated using the program MODELER (19) and the QUANTA/CHARMm package (Molecular Simulations Inc). The heme was docked into the model based on the coordinates of CYP 107A and then energy minimized using CHARMm to alleviate steric clashes. The structure was evaluated by several methods to determine the validity of the model. The model was checked with PROCHECK (20) to evaluate the stereochemical quality of the model. Residue packing and environments were examined using Whatif Quality Control (21). The surfaces and volumes of the structure were evaluated using SURVOL (22).

The volumes of the active site cavities were calculated using the program VOIDOO (23) for CYP119, CYP101 and CYP102. The substrate free structure of CYP101 was used (16) and averages were taken for the two substrate free structures of CYP102 (17, 24). CYP102 crystallized with two molecules in the asymmetric unit, and hence for these calculations the two molecule 1 structures were averaged (open conformation) and the two molecule 2 structures were averaged (closed conformation) separately. The volumes were calculated using a probe radius of 1.4 Å.

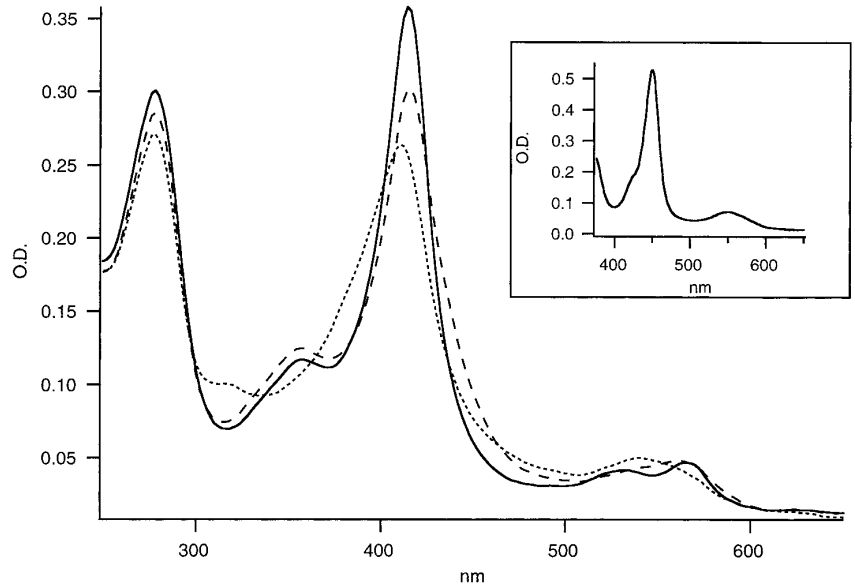

FIG. 1. UV/Visible spectra for CYP119 in the ferric low spin (—), reduced (- - -), and oxy bound (– –) states. The insert shows the characteristic CO bound 450 spectra.

RESULTS

The thermostability of CYP119 allows for a heat denaturation step in which >50% of the *E. coli* proteins present denature. Following this with an ammonium sulfate precipitation (30–50%), a size exclusion column, and an HPLC anion exchange column gives rise to protein which purifies to homogeneity.

The UV-VIS optical spectra are presented in Fig. 1. The substrate free oxidized form of the protein shows a Soret maximum at 415 nm (ϵ = 104 mM^{-1}) similar to that of P450 (CYP101) (417 nm) and visible bands at 533 (ϵ = 10.8 mM^{-1}) and 566 nm (ϵ = 12.0 mM^{-1}). In the reduced form the Soret band blue shifts to 410 nm which is identical to other known P450s and the visible band is located at 540 nm. After oxygenation of the reduced form results in a Soret band near 416 nm, but it is hard to distinguish the exact location since autooxidation proceeds too quickly to form a clean oxidized spectra. The CO bound form of the enzyme displays a characteristic Soret maximum of 450 nm with a visible band at 550 nm.

Figure 2 shows the DSC scans for substrate free cytochrome P450 CYP101 and CYP119. The T_m for CYP101 is centered at 54°C while that of CYP119 is centered at 91°C. Both transitions are irreversible mainly due to the loss of the heme moiety.

The stability of CYP119 toward hydrostatic pressure is shown in Fig. 3. It is seen that up to 2 kbar there is little change in the amount of P450 present while in the case of P450 CYP101 at 2 kbar there is little or no native P450 left.

In order to probe the active site we compared the CO flash photolysis geminate yields of CYP119, CYP101, and CYP102 in the substrate free form. Previous studies have shown that active site volume can be correlated with the geminate yield which is operationally defined as the fraction of photolyzed CO remaining in the active site prior to rebinding. A typical trace for CYP119 is shown in Fig. 4. The geminate yields and

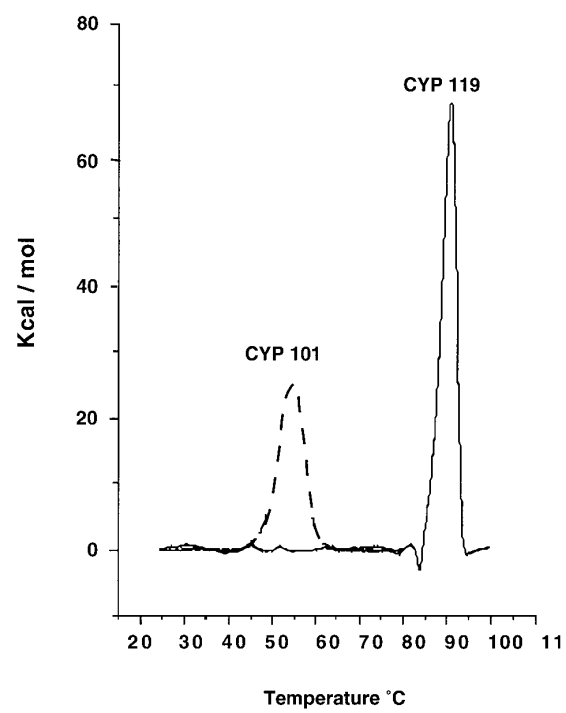

FIG. 2. 2 DSC scans for CYP119 (—) and CYP102 (– –). Scans were taken with a scan rate of 70°C/hr from 25 to 100°C for CYP119 and 25 to 80°C for CYP102.

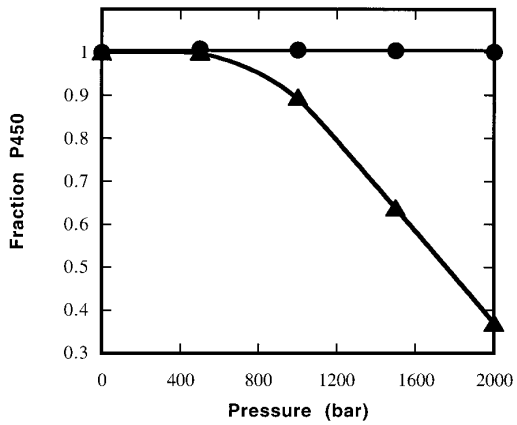

FIG. 3. The fraction of native P450 versus pressure for CYP119 (●) and CYP101 (▲) are shown as calculated by the absorbance at 450 nm in the ferrous carbonyl adduct relative to that at ambient pressure.

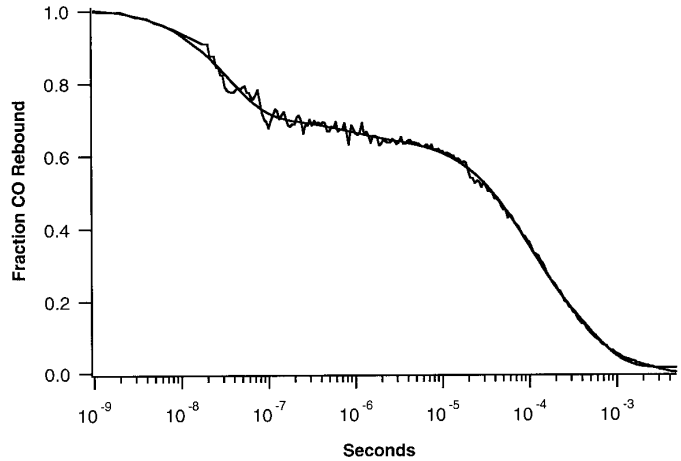

FIG. 4. CO rebinding transient for CYP119 after flash photolysis. A Spectra Physics GCR 150 Nd:YAG laser which produces a 200-mJ pulse with a duration of 7 ns at 532 nm was used for photolysis.

active site volumes as calculated by VOIDOO are listed in Table 1 and display a trend in which the fraction of CO exiting the pocket increases as active site volume increases. Calculations of the active site cavity of the more open molecule in the asymmetric unit of the crystal structure of CYP102 were impossible because the cavity opened into the solvent exposed surface.

DISCUSSION

We have successfully cloned and isolated CYP119 from *Sulfolobus solfataricus.* This P450 exhibits extreme stability to both temperature (T_m = 91°C) and pressure (>2 kbar). The characteristic UV-VIS optical and EPR (data not shown) spectra confirm that the polypeptide sequence is indeed a cytochrome P450, thus confirming the presence of cytochrome P450s in the archaea phylogenetic domain.

The substrate of CYP119 remains elusive, however some insights about the appearance of its active sight can be drawn from the results of the homology modeling in conjunction with CO flash photolysis experiments. General inspection of the homology model shows that the heme binding region is in tact with the heme ligated to the Cys 317. The active site contains the conserved acid-threonine pair shown on the left side of Fig. 5. From the model, the active site appears to have a more hydrophobic region and a region that appears more polar, suggesting that the substrate may be a hydrophobic substrate with a polar substituent localized to one portion of the ligand.

Further characterization of the active site is provided from the results of the flash photolysis experiments which suggest that the active site pocket may be more open and solvent accessible. Previous work has shown that the geminate yield can be correlated with the active site volume by the decreased geminate yield as the active site becomes more accessible to the surface with a correspondingly greater chance for the CO to escape (12).

Obviously an important goal of this work is to understand the differences between CYP119 and the other known P450s which convey overall stability to thermal or pressure perturbations. As described in the introduction of this manuscript, there have been many suggestions as to the origins of thermo- and barostability. Each of these has been examined for CYP119 and, although none of them seem to be able to completely explain the observed stability, several correlations can be noted.

One factor shown to contribute to protein thermostability is increased percentage of hydrophobic residues, presumably corresponding to an increased buried core of the protein. While it appears that there may be regions of CYP119 which may be more enriched in hydrophobic residues, the overall percent of hydrophobic residues is in the range with that of other P450's.

Another type of interaction which may contribute to the stability is the aromatic stacking. Inspection of the homology model shows clustering of hydrophobic residues similar to the cluster found in the P2 protein (4), centering around Trp 281 (Fig. 6). Increased hydro-

TABLE 1

	Fraction CO leaving pocket	Active site volume (Å^3)
CYP 102	70%[a]	343
CYP 119	64%	223
CYP 101	10%[b]	79

[a] Ref. 11.
[b] Ref. 24.

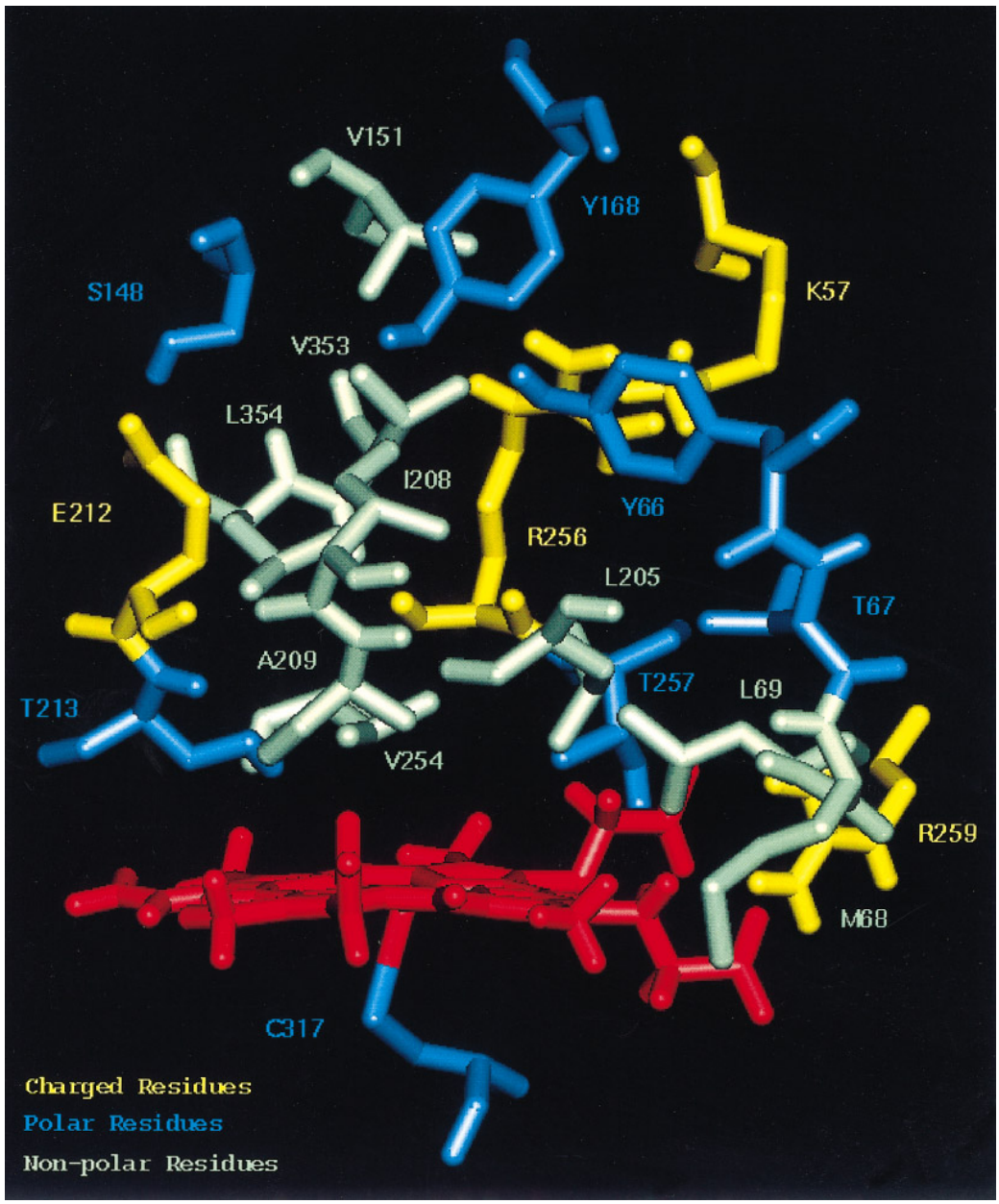

FIG. 5. The active site of the modeled CYP119 displaying all of the residues surrounding the open heme pocket. The charged residues are yellow, the polar residues are blue, the nonpolar residues are light green and the heme is red.

static pressure favors the aromatic stacking interactions due to their smaller volumes. While it is impossible to quantitate the effect of this interaction, qualitatively the aromatic residues appear to cluster more in CYP119 than the four other known P450 structures. This interaction may have important contributions to the thermo- and/or barostability.

While other suggestions such as an increased number of salt bridges and higher percentage of buried residues versus solvent accessible residues has been suggested, none of these seem to play a clear role when examining the modeled CYP119 structure. It may be that there are several subtle differences which additively comprise the large stability increase for CYP119. It is clear that more investigations, including studies with site directed mutants will be necessary to obtain a more accurate picture of the interactions essential for conveying the extreme thermo- and barostability.

CONCLUSION

We have cloned and isolated a cytochrome P450 (CYP119) from the thermophilic archaea *Sulfolobus*

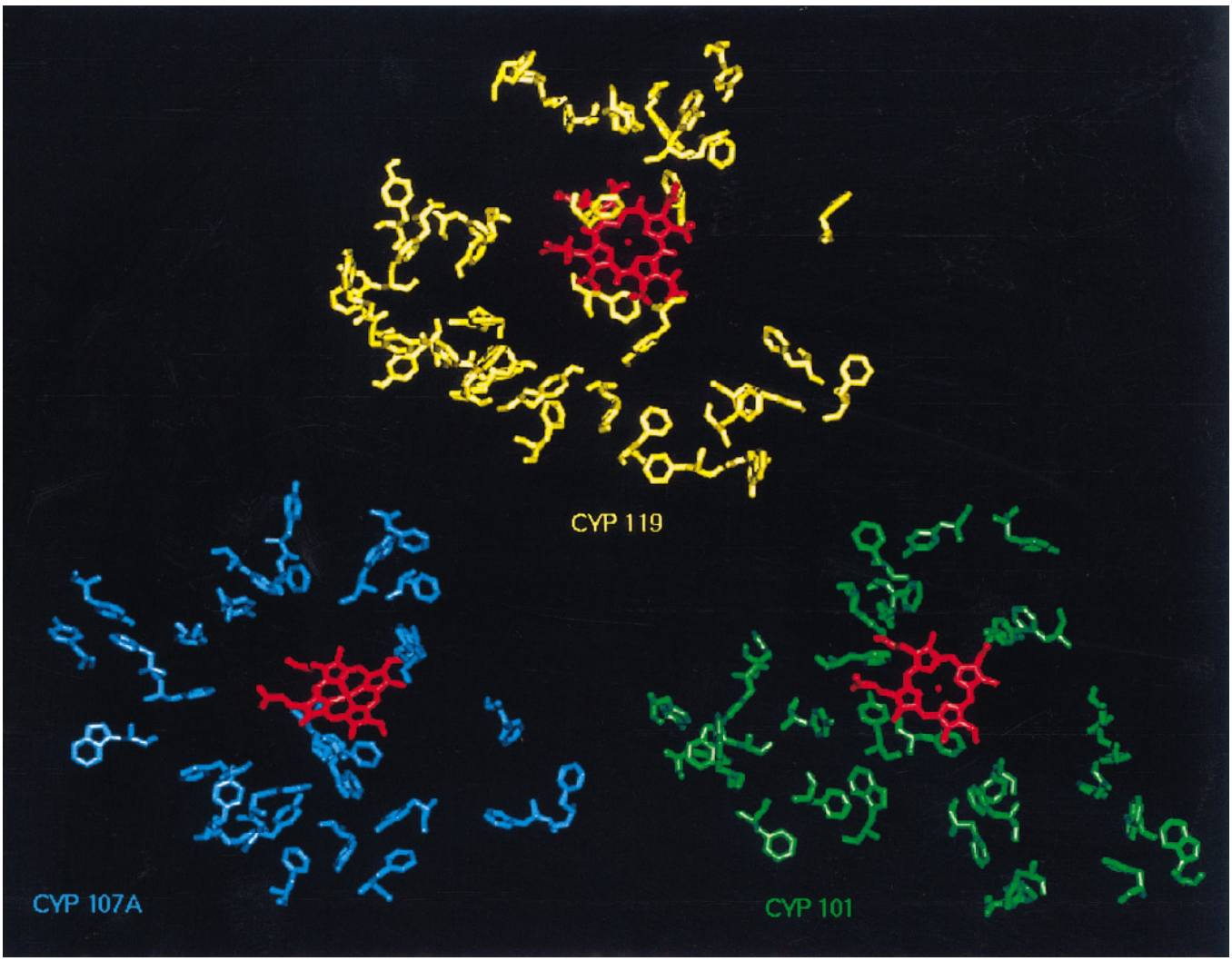

FIG. 6. The aromatic residues (Phe, Trp, and Tyr) are shown for the model of CYP119, and structures of CYP 107A(14) and CYP101(16). The aromatic residues shown are more clustered and form aromatic stacking interactions in CYP119 compared to CYP101.

solfataricus. This enzyme exhibits thermo- and barostability unprecedented in the P450 family of enzymes. Homology modeling suggest that the active site is similar to known P450s and that the pocket may be characterized as more open and somewhat more polar. Although the function of this enzyme is not yet known, the features of its stability may give insight into generating other highly stable P450s with desired activities (25). Experiments are currently in progress to provide a complete thermodynamic characterization as well as the search (25) for its redox partners.

ACKNOWLEDGMENTS

This work is supported by NIH Grants GM 33775 and GM 31756. We thank Dr. Gary Olsen and David Graham for valuable discussions regarding the growth of *Ss.* We also thank Aretta Weber for excellent help in manuscript preparation. S. Maves is supported by a Molecular Biophysics Training grant from the National Institutes of Health.

REFERENCES

1. Guengerich, F. P., and Macdonald, T. L. (1990) *FASEB J.* **4,** 2453–2459.
2. Wright, R. L., Harris, K., Solow, B., White, R. H., and Kennelly, P. J. (1996) *FEBS Lett.* **384,** 235– 239.
3. D'Auria, S., Rossi, M., Barone, G., Catanzano, F., Vecchio, P. D., Graziano, G., and Nucci, R. (1996) *J. Biochem.* **120,** 292–300.
4. Fusi, P., Goossens, K., Consonni, R., Grisa, M., Puricelli, P., Vecchio, G., Vanoni, M., Zetta, L., Haremans, K., and Tortora, P. (1997) *Proteins Stuct. Funct. Gen.* **29,** 381–390.
5. Russo, A. D., Rullo, R., Nitti, G., Masullo, M., and Bocchini, V. (1997) *Biochim. Biophys. Acta* **1343,** 23–30.
6. Hamon, V., Dallet, S., and Legoy, M.-D. (1996) *Biochim. Biophys. Acta* **1294,** 195–203.
7. Bec, N., Villa, A., Tortora, P., Mozhaev, V. V., Balny, C., and Lange, R. (1996) *Biotech. Lett.* **18,** 483–488.
8. Maniatis, T., Fritsch, E. F., Sambrook, J. (1989) Molecular Cloning: A Laboratory Manual, Cold Spring Harbor Laboratory Press, Cold Spring Harbor, NY.

9. Omura, T., and Sato, R. (1964) *J. Biol. Chem.* **239,** 2370– 2378.
10. Gerber, N. C., and Sligar, S. G. (1994) *J. Biol. Chem.* **269,** 4260–4266.
11. Paladini, A. A., and Weber, G. (1981) *Rev. Sci. Instrum.* **52,** 419–427.
12. Mclean, M. A., Yeom, H., and Sligar, S. G. (1996) *Biochime* **78,** 700–705.
13. Tetreau, C., Di Primo, C., Lange, R., Tourbez, H., and Lavalette, D. (1997) *Biochemistry* **36,** 10262–10275.
14. Cupp-Vickery, J. R., and Poulos, T. L. (1995) *Nat. Struct. Biol.* **2,** 144–153.
15. Hasemann, C. A., Ravichandran, K. G., Peterson, J. A., and Diesenhofer, J. (1994) *J. Mol. Biol.* **236,** 1169–1185.
16. Poulos, T. L., Finzel, B. C., and Howard, A. J. (1986) *Biochemistry* **25,** 5314–5322.
17. Ravichandran, K. G., Bouddupalli, S. S., Hasemann, C. A., Peterson, J. A., and Deisenhofer, J. (1993) *Science* **261,** 731–736.
18. Thompson, J. D., Higgins, D. G., and Gibson, T. J. (1994) *Nucleic Acids Res.* **22,** 4673–4680.
19. Sali, A., and Blundell, T. L. (1993) *J. Mol. Biol.* **234,** 779–815.
20. Laskowski, R. A., MacArthur, M. W., Moss, D. S., and Thornton, J. M. (1993) *J. Appl. Cryst.* **26,** 283–291.
21. Hooft, R. W. W., Vriend, G., Sander, C., and Abola, E. E. (1996) *Nature* **381,** 272.
22. Wodak, S. J., Pontius, J., Vaguine, A., and Richelle, J. (1995) *in* Making the Most of Your Model, Proceedings of the CCP4 Study Weekend, pp. 6–7.
23. Kleywegt, G. J., and Jones, T. A. (1994) *Acta Cryst.* **D50,** 178–185.
24. Li, H., and Poulos, T. L. (1995) *Acta. Cryst.* **D51,** 21–32.
25. Tian, W. D., Wells, A. V., Champion, P. M., Di Primo, C., Gerber, N., and Sligar, S. (1995) *J. Biol. Chem.* **270,** 8673–8679.